ARTICLE

BIOTECHNOLOGY and BIOENGINEERING

Aldehyde–Alcohol Dehydrogenase and/or Thiolase Overexpression Coupled With CoA Transferase Downregulation Lead to Higher Alcohol Titers and Selectivity in *Clostridium acetobutylicum* Fermentations

Ryan Sillers,[1] Mohab Ali Al-Hinai,[2] Eleftherios T. Papoutsakis[1,3]

[1]Department of Chemical and Biological Engineering, Northwestern University, Evanston, Illinois 60208; telephone: 302-831-8376; fax: 302-831-4841; e-mail: epaps@udel.edu

[2]Biology Department, College of Science, Sultan Qaboos University, Muscat, Oman

[3]Department of Chemical Engineering & The Delaware Biotechnology Institute, University of Delaware, 15 Innovation Way, Newark, DE 19716.

Received 11 May 2008; revision received 14 July 2008; accepted 15 July 2008

Published online 22 July 2008 in Wiley InterScience (www.interscience.wiley.com). DOI 10.1002/bit.22058

ABSTRACT: Metabolic engineering (ME) of *Clostridium acetobutylicum* has led to increased solvent (butanol, acetone, and ethanol) production and solvent tolerance, thus demonstrating that further efforts have the potential to create strains of industrial importance. With recently developed ME tools, it is now possible to combine genetic modifications and thus implement more advanced ME strategies. We have previously shown that antisense RNA (asRNA)-based downregulation of CoA transferase (CoAT, the first enzyme in the acetone-formation pathway) results in increased butanol to acetone selectivity, but overall reduced butanol yields and titers. In this study the alcohol/aldehyde dehydrogenase (*aad*) gene (encoding the bifunctional protein AAD responsible for butanol and ethanol production from butyryl-CoA and acetyl-CoA, respectively) was expressed from the phosphotransbutyrylase (*ptb*) promoter to enhance butanol formation and selectivity, while CoAT downregulation was used to minimize acetone production. This led to early production of high alcohol (butanol plus ethanol) titers, overall solvent titers of 30 g/L, and a higher alcohol/acetone ratio. Metabolic flux analysis revealed the likely depletion of butyryl-CoA. In order to increase then the flux towards butyryl-CoA, we examined the impact of thiolase (THL, *thl*) overexpression. THL converts acetyl-CoA to acetoacetyl-CoA, the first step of the pathway from acetyl-CoA to butyryl-CoA, and thus, combining *thl* overexpression with *aad* overexpression decreased, as expected, acetate and ethanol production while increasing acetone and butyrate formation. *thl* overexpression in strains with asRNA CoAT downregulation did not significantly alter product formation thus suggesting that a more complex metabolic engineering strategy is necessary to enhance the intracellular butyryl-CoA pool and reduce the acetyl-CoA pool in order to achieve improved butanol titers and selectivity.

Biotechnol. Bioeng. 2009;102: 38–49.

KEYWORDS: *Clostridium acetobutylicum*; metaboli engineering; thiolase; flux analysis; acetyl-CoA; butyryl-CoA

Introduction

Recent advances in molecular biology and metabolic engineering (ME) techniques of butyric-acid clostridia offer an opportunity to re-establish the acetone, butanol, and ethanol (ABE) fermentation as an economically viable process. *Clostridium acetobutylicum* is a model and prototypical organism for the production of these commodity chemicals, and especially that of butanol, which has now emerged as an important new biofuel. The genome of *C. acetobutylicum* has been sequenced and annotated (Nölling et al., 2001), and methods for genetic deletions (Harris et al., 2002; Heap et al., 2007; Shao et al., 2007) and gene overexpression (Mermelstein and Papoutsakis, 1993) have been developed. Furthermore, genome-scale microarray-based transcriptional analyses (Alsaker and Papoutsakis, 2005; Alsaker et al., 2004, 2005; Tomas et al., 2003a,b)

Correspondence to: E.T. Papoutsakis

Contract grant sponsor: National Science Foundation

Contract grant number: BES-0418157

Additional Supporting Information may be found in the online version of this article.

have illuminated its complex metabolism, thus allowing the development of more precise ME strategies, by combining genetic modifications. Here we address ME issues related to flux determinism in core primary-metabolism pathways.

High butanol selectivity and titers in the ABE fermentation are current obstacles for an economical industrial process. Butanol is the most valuable product, and thus the production of all other products must be minimized. Ethanol is the only other product that may be desirable as a co-product in the context of biofuel production. The ABE batch fermentation is characterized by two distinct phases, the acidogenic and the solventogenic phase. Initially, the cultures produce the organic acids butyrate and acetate, which lowers the culture pH. In the solventogenic phase, the culture produces butanol, acetone, and ethanol. Butyrate and acetate are partially re-assimilated to produce solvents, thus raising the pH of the culture. The trigger responsible for the switch from acid to solvent formation (known as solventogenesis) has been extensively studied, but the exact mechanism for this change remains unknown. The external pH is known to affect solventogenesis and product formation (Husemann and Papoutsakis, 1988). Recent evidence correlates increases of butyryl-phosphate (BuP) concentration with the onset of solvent formation and suggests that BuP may play a role in the regulation of solvent initiation (Zhao et al., 2005).

In wildtype (WT) *C. acetobutylicum* fermentations, final acetone concentrations are typically one-half the final levels of butanol. Initial efforts to increase the selectivity of butanol to acetone used antisense RNA (asRNA) technology targeting the transcripts of enzymes in the acetone formation pathway (Fig. 1). The *ctfB* asRNA successfully reduced acetone production when designed to downregulate a subunit of the first enzyme in the acetone formation pathway, CoA transferase (CoAT) (Tummala et al., 2003b). However, butanol titers were also significantly reduced in the *ctfB* asRNA strain. The *ctfB* gene is part of a tricistronic operon (*aad-ctfA-ctfB*) also containing the *aad* gene, whose product, the bi-functional AAD (alcohol/aldehyde dehydrogenase) protein, catalyzes the two-step conversion of butyryl-CoA to butanol or of acetyl-CoA to ethanol (Nair et al., 1994). Because the *ctfB* and *aad* genes reside on the same mRNA transcript, the *ctfB* asRNA resulted in a downregulation of both the *ctfB* and *aad* genes thus resulting in lower butanol production (Tummala et al., 2003b). Follow-up studies were able to restore WT butanol titer levels while maintaining low acetone production by combining, in strain 824(pAADB1) the *ctfB* asRNA with the overexpression of the *aad* gene alone off plasmid pAADB1 using its own autologous promoter (Tummala et al., 2003a). Significantly, this strain produced ca. 200 mM ethanol, the highest ever in *C. acetobutylicum*. The high ethanol production is due to the dual functionality of the AAD enzyme, which catalyzes both the formation of ethanol and butanol. In the WT strain, butanol is produced nearly sixfold higher than ethanol. The logical and accepted interpretation is that AAD has a much higher affinity for butyryl-CoA than for acetyl-CoA (Fig. 1).

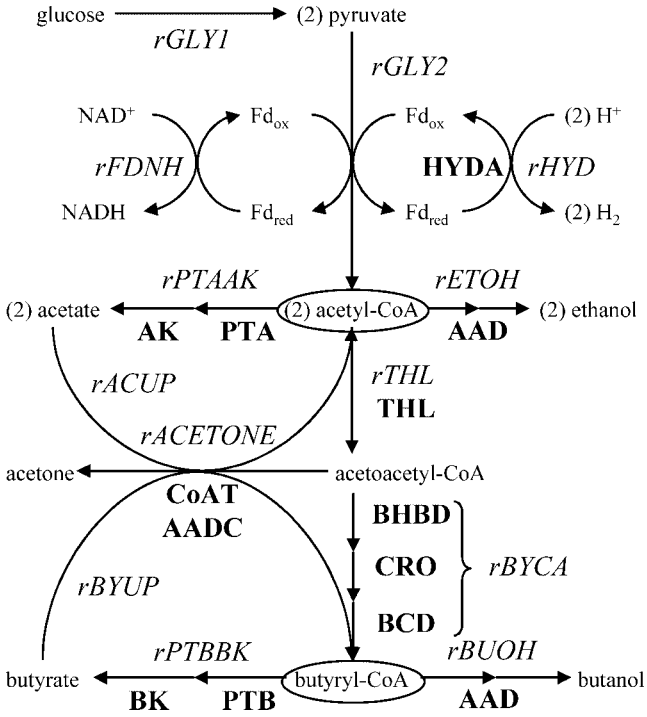

Figure 1. Metabolic pathways in *C. acetobutylicum* and associated calculated in vivo fluxes. Selected enzymes are shown in bold and associated intracellular fluxes are shown in italics. The metabolic intermediates acetyl-CoA and butyryl-CoA are in ovals to highlight their importance in final product formation. Enzymes are abbreviated as follows: hydrogenase (HYDA); phosphotransacetylase (PTA); acetate kinase (AK); thiolase (THL); β-hydroxybutyryl dehydrogenase (BHBD); crotonase (CRO); butyryl-CoA dehydrogenase (BCD); CoA Transferase (CoAT); acetoacetate decarboxylase (AADC); butyrate kinase (BK); phophotransbutyrylase (PTB); alcohol/aldehyde dehydrogenase (AAD). Note: AAD is believed to be the primary enzyme for butanol and ethanol formation but additional genes exist that code for alcohol forming enzymes (*adhe2, bdhA, bdhB*, CAC3292, CAP0059).

The high ethanol production by strain 824(pAADB1) suggests that the ratio of acetyl-CoA to butyryl-CoA is much higher in this strain than in the WT strain. In this study we aimed to explore ME strategies to enhance butanol formation and selectivity and, significantly, to be able to accelerate butanol production. We focused on exploring the regulation of fluxes around the two critical nodes of butyryl-CoA and acetyl-CoA (Fig. 1). First, we sought to overexpress *aad* (AAD) early by changing the temporal expression of this gene using the *ptb* promoter (of the *ptb-buk* operon, coding the two enzymes responsible for butyrate production from butyryl-CoA; Fig. 1) which is expressed early in the acidogenic growth phase (Tummala et al., 1999) when the *aad* natural expression is normally absent (Nair et al., 1994). This early expression of *aad* sought to direct more of the carbon flux towards butanol production while limiting the formation of butyrate by competing early for butyryl-CoA. The possibility of reducing ethanol and acetate production by altering the fluxes around the acetyl-CoA node focusing

on the overexpression of the thiolase gene (Fig. 1) was also investigated.

Materials and Methods

Bacterial Stains and Plasmids

The list of bacterial strains and plasmids are in Table I.

Culture Conditions

E. coli strains were grown aerobically at 37°C and 200 rpm in liquid LB media or solid LB with agar (1.5%) media supplemented with the appropriate antibiotics (ampicillin at 50 μg/mL or chloramphenicol at 35 μg/mL). Frozen stocks were made from 1 mL overnight culture resuspended in LB containing 15% glycerol and stored at −85°C. *C. acetobutylicum* strains were grown anerobically at 37°C in an anaerobic chamber (Thermo Forma, Waltham, MA). Cultures were grown in liquid CGM (containing 0.75 g KH_2PO_4, 0.982 g K_2HPO_4, 1.0 g NaCl, 0.01 g $MnSO_4$, 0.004 g *p*-aminobenzoic acid. 0.348 g $MgSO_4$, 0.01 g $FeSO_4$, 2.0 g asparagine, 5.0 g yeast extract, 2.0 g $(NH_4)_2SO_4$, and 80 g glucose, all per liter) media or solid 2× YTG pH 5.8 (containing 16 g Bacto tryptone, 10 g yeast extract, 4 g NaCl, and 5 g glucose, all per liter) plus agar (1.5%) supplemented with antibiotics as necessary (erythromycin at 100 μg/mL in liquid media and 40 μg/mL in solid media, clarithromycin at 75 μg/mL). Cultures were heat shocked at 70–80°C for 10 min to enhance solvent production and prevent strain degeneration (Cornillot et al., 1997). Frozen stocks were made from 10 mL of A_{600} 1.0 culture resuspended in 1 mL CGM containing 15% glycerol and stored at −85°C.

Plasmid and Strain Construction

The *aad* gene (CAP0162) responsible for butanol formation was PCR amplified from *C. acetobutylicum* genomic DNA using primers aad_fwd and aad_rev to exclude the natural promoter. All primers used in plasmid construction are listed in Supplementary Table I. The pSOS94 vector was digested with *Bam*HI and *Ehe*I and blunt ended to remove the acetone formation genes while leaving the *ptb* promoter region and the *adc* terminator. The *aad* PCR product and the linearized pSOS94 vector were ligated to create pPTBAAD. Both pCTFB1AS, containing the *ctfB* asRNA, and pPTBAAD were digested with *Sal*I to linearize pCTFB1AS and isolate the *aad* gene with the *ptb* promoter and *adc* terminator from pPTBAAD. These fragments were ligated together to generate pCASAAD.

The thiolase (*thl*) gene including the endogenous promoter and terminator regions was amplified from *C. acetobutylicum* genomic DNA using primers thl_fwd and thl_rev. Following purification, the PCR product was digested with *Sal*I and *Eco*RI as was the shuttle vector pIMP1. The digested PCR product was ligated into the pIMP1 shuttle vector to form the plasmid pTHL. The *aad* gene cassette from pPTBAAD was isolated using an *Sal*I digestion and purified. Plasmid pTHL was *Sal*I digested and ligated with the purified *aad* gene cassette to generate plasmid pTHLAAD.

Table I. Bacterial stains and plasmids used in this study.

Strain or plasmid	Relevant characteristics[a]	Source or references[b]
Bacterial strains		
C. acetobutylicum		
ATCC 824		ATCC
M5		Clark et al. (1989)
E. coli		
Top10		Invitrogen
ER2275		New England Biolabs
Plasmids		
pAN1	Cm^r, Φ3T I gene, p15A origin	Mermelstein and Papoutsakis (1993)
pSOS94[c]	Acetone operon (*ptb* promoter)	Soucaille and Papoutsakis, unpublished
pCTFB1AS[c]	*ctfB* asRNA (*thl* promoter)	Tummala et al. (2003b)
pCASAAD[c]	*aad*, (*ptb* promoter), *ctfB* asRNA (*thl* promoter)	This study
pAADB1[c]	*aad*, (*aad* promoter), *ctfB* asRNA (*thl* promoter)	Tummala et al. (2003a)
pTHL[c]	*thl* (*thl* promoter)	This study
pTHLAAD[c]	*thl*, *aad*, (*ptb* promoter)	This study
pPTBAAD[c]	*aad*, (*ptb* promoter)	This study
pCAS[c]	*ctfB* asRNA (*adc* promoter)	This study
pSOS95del[c]	*thl* promoter only	Tummala et al. (2003a)
pSS2[c]	*aad*, (*ptb* promoter), *ctfB* asRNA (*adc* promoter), *thl*	This study

[a]Cm^r, chloramphenicol resistance gene; *ptb*, phosphotransbutyrylase gene; *aad*, alcohol/aldehyde dehydrogenase gene; *ctfB*, CoA transferase subunit B gene; *thl*, thiolase gene; *adc*, acetoacetate decarboxylase gene.
[b]ATCC, American Tissue Culture Collection, Rockville, MD.
[c]Contains the following: ampicillin resistance gene; macrolide, lincosimide, and streptogramin B resistance gene; *repL*, pIM13 Gram-positive origin of replication; ColE1 origin of replication.

A revised *ctfB* asRNA cassette was generated by first inserting a 100 bp oligonucelotide into the pIMP1 shuttle vector following digestion with *Sal*I and *Eco*RI. This oligonucleotide includes the sequence for the *adc* promoter element with compatible nucleotide overhangs for ligation. The complimentary oligonucleotides p_adc_top and p_adc_bot were first annealed together before ligating into the pIMP1 vector, creating pPADC, which was then digested with *Eco*RI and *Nde*I. A second set of complementary oligonucleotides, ctfBas_top and ctfBas_bot, were annealed and ligated to the digested pPADC to form pCAS. The new *ctfB* asRNA cassette was PCR amplified from this plasmid using primers cas_fwd and cas_rev and ligated into the pTHLAAD plasmid to generate plasmid pSS2.

All plasmids were transformed into Top 10 chemically competent *E. coli* (Invitrogen, Carlsbad, CA). Plasmids were confirmed using sequencing reactions. The plasmids were methylated using *E. coli* ER2275 (pAN1) cells to avoid the natural restriction system of *C. acetobutylicum* (Mermelstein and Papoutsakis, 1993). Once methylated, the plasmids were transformed by electroporating *C. acetobutylicum* wildtype (WT) or mutant M5 strains as described (Mermelstein et al., 1992).

Bioreactor Experiments

Fermentations were carried out using a BioFlo 110 or BioFlo II (New Brunswick Scientific Co., Edison, NJ) bioreactor with 4.0 L working volumes. Fermentations used a 10% (v/v) inoculum of a pre-culture with A_{600} equal to 0.2. CGM media were supplemented with 0.10% (v/v) antifoam and 75 μg/mL clarithromycin. Fermentations were maintained at constant pH using 6 M NH_4OH. Anaerobic conditions were maintained through nitrogen sparging. Temperature was maintained at 37°C and agitation was set at 200 rpm. Glucose was restored to the initial concentration (440 mM) in fermentations if glucose levels fell below 200 mM. Glucose was added to 824(pCASAAD) at hour 29, to 824(pTHLAAD) at hour 23, and to 824(pAADB1) at hour 64.

Analytical Techniques

Cell density was measured at A_{600} using a Biomate3 spectrophotometer (Thermo Spectronic, Waltham, MA). Samples were diluted as necessary to keep absorbance below 0.40. Products and glucose were analyzed by HPLC as previously reported (Alsaker and Papoutsakis, 2005).

RNA Sampling and Isolation

Cell pellets from 3 to 10 mL of culture were incubated at 37°C for 4 min in 200 μL of SET buffer (25% sucrose, 50 mM EDTA pH 8.0, 50 mM Tris–HCl pH 8.0) with 20 mg/mL lysozyme. 1 mL trizol was added to each sample and stored at −85°C until purification. 0.5 mL trizol and 0.2 mL chloroform was added to 0.5 mL RNA sample and centrifuged at 12,000 rpm for 15 min. The aqueous phase was collected and added to an equal volume of isoproponal and RNA was precipitated at 12,000 rpm for 10 min. One milliliter ethanol was added to wash the pellet and centrifuged at 9,500 rpm for 4 min. Samples were dried and resuspended in 20–100 μL of RNase free water and stored at −85°C.

Quantitative (Q)-RT-PCR

Reverse transcription of RNA was carried out using random hexamer primers with 500 μM dNTPs, 2.0 μg RNA, 2 μL RNase inhibitor, 2.5 μL reverse transcriptase, and 2.5 μM random hexamers in a total volume of 100 μL (Applied Biosystems, Foster City, CA). The reaction was incubated at 25°C for 10 min, 48°C for 30 min, followed by inactivation of the enzymes by a 5-min incubation at 95°C. The SYBR green master mix kit (Applied Biosystems) was used for RT-PCR. Each PCR contained 1 μL cDNA and 1 μM gene specific primers (Supplementary Table I) in a total volume of 25 μL. Samples were performed in triplicate on a BioRad iCycler with the following parameters: 10 min at 95°C, 40 cycles of 15 s at 95°C and 1 min at 60°C. All genes were normalized to the pullulanase gene (Tomas et al., 2003c).

Metabolic Flux Analysis

Metabolic Flux analysis calculations were performed using a program developed by Desai et al. (1999b). Product concentrations from bioreactor experiments were used to generate metabolic fluxes. Error associated with the calculated fluxes is typically less than 10% (Desai et al., 1999a,b; Harris et al., 2000). The metabolic network is shown in Figure 1, with associated fluxes shown in italics.

Results

Early and Elevated Expression of *aad* Using the *ptb* Promoter

We aimed to explore ME strategies to enhance butanol formation and selectivity and accelerate butanol production. We focused on exploring the regulation of fluxes around the two critical nodes of butyryl-CoA and acetyl-CoA (Fig. 1). First, we sought to enhance and accelerate butanol and ethanol production by increasing the expression of the enzyme responsible for butanol and ethanol formation, alcohol/aldehyde dehydrogenase (AAD) (Fig. 1). This was accomplished by changing the temporal expression of this gene using the *ptb* promoter, p_{ptb} (of the *ptb-buk* operon, coding the two enzymes responsible for butyrate production from butyryl-CoA; using plasmid pPTBAAD), which is active early in the acidogenic growth phase (Tummala et al., 1999) when the *aad* natural expression is normally absent

(Nair et al., 1994). This early expression of *aad* sought to direct more of the carbon flux towards butanol production while limiting the formation of butyrate by competing early for butyryl-CoA. It was expected that the early-plasmid expressed *aad* with the later chromosomal expressed *aad* from its natural promoter would make possible the sustained butanol production throughout both the acidogenic and solventogenic growth phases. pPTBAAD was first transformed into the degenerate strain M5 (which has lost the pSOL1 megaplasmid and thus the ability to express the *sol* operon and form butanol or acetone (Cornillot et al., 1997)) to confirm the proper expression of *aad* and the production of a functional protein. Production of butanol in M5(pPTBAAD) was observed (results not shown) confirming expression and translation of *aad* from p_{ptb}. Then, *aad* expressed from the p_{ptb} was isolated from pPTBAAD and combined into a plasmid containing the *ctfB* asRNA, creating plasmid pCASAAD. Following the transformation of pCASAAD into the WT strain, controlled pH 5.0 fermentations were performed in duplicate to fully characterize the 824(pCASAAD) compared to the strain containing the *ctfB* asRNA and *aad* overexpression from its endogenous promoter, 824(pAADB1), and the plasmid control strain containing only the thiolase promoter without the *ctfB* asRNA and without *aad* overexpression, 824(pSOS95del) (Fig. 2).

RNA samples were collected during the fermentations and analyzed for the level of *aad* expression using Q-RT PCR. Comparing the *aad* expression between the strains, there exists a nearly 10-fold higher expression of *aad* in 824(pCASAAD) than in 824(pAADB1) during the first four timepoints (Fig. 2). These timepoints correspond to the exponential growth phase and the early transitional phase when the p_{ptb} is expected to have the highest activity. During the later timepoints, *aad* expression continues to be higher in 824(pCASAAD), but at lower levels than initially observed. Expression of *aad* within each strain was also examined. In 824(pCASAAD), *aad* expression is highest

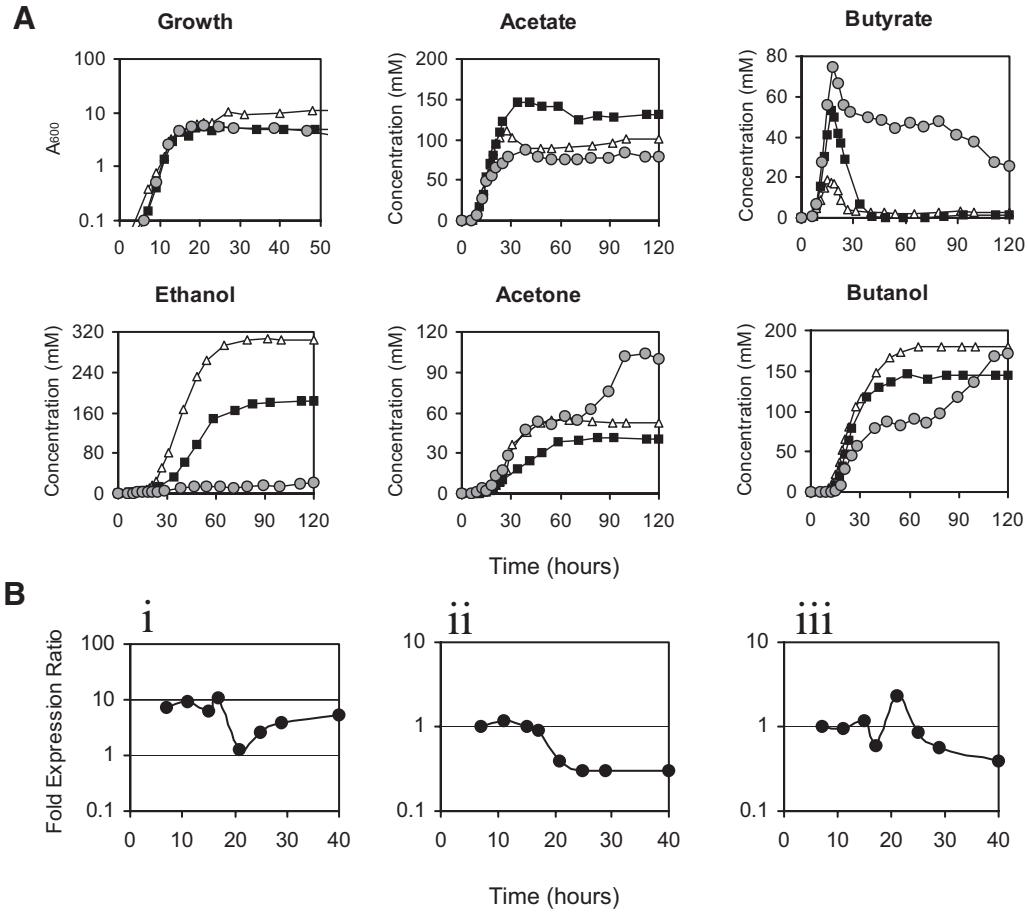

Figure 2. Growth and product concentrations of 824(pCASAAD), 824(pAADB1) and 824(pSOS95del) pH 5.0 fermentations, and Q RT-PCR analysis of *aad* expression. Fermentations were performed in duplicate, while results are shown from one fermentation. Differences in product formation between duplicate fermentations are less than 5%. Lag times were standardized between fermentations by normalizing an A_{600} of 1.0 at hour 10 of the fermentation. **A**: 824(pCASAAD) results are shown as open triangles, 824(pAADB1) results are shown as closed squares, and 824(pSOS95del) results are shown as gray circles. **B**: For Q RT-PCR analysis of *aad* expression, samples were taken from the bioreactor experiments of (A) above. (i) Ratio of *aad* expression in 824(pCASAAD) relative to 824(pAADB1) comparing similar timepoints. (ii) Ratio of *aad* expression in 824(pCASAAD) relative to the first timepoint sampled. (iii) Ratio of *aad* expression in 824(pAADB1) relative to the first timepoint sampled.

during the first four timepoints after which the expression level decreases. This pattern is opposite that in the WT strain whereby *aad* expression is absent early, but is later induced in the stationary phase (Alsaker and Papoutsakis, 2005). This shows that the p_{ptb} was successful in enhancing the early expression of *aad*. The pattern of *aad* expression in 824(pAADB1) is more complex. There exists a distinct peak in expression of *aad* that corresponds to the entry into stationary phase, when *aad* is induced in the WT strain. After this point, the *aad* expression begins to decrease.

ptb-Promoter-Driven *aad* Expression Leads to Higher Cell Densities and Increased, Earlier Butanol Formation

Although the growth rate was similar between all strains, 824(pCASAAD) reached higher cell densities (Table II) than either 824(pAADB1) or 824(pSOS95del). We attributed these higher cell densities to the lower butyrate concentrations observed in 824(pCASAAD) (Fig. 2): butyrate was completely re-assimilated by both strains with the *ctfB* asRNA, but peak butyrate levels were reduced by two-thirds in 824(pCASAAD) compared to 824(pAADB1). Furthermore, both the peak and final acetate levels were reduced in 824(pCASAAD) compared to 824(pAADB1): final acetate concentrations were 129 mM in 824(pAADB1), 85 mM in 824(pCASAAD) and 77 mM in the plasmid control strain 824(pSOS95del). Solvent formation shows significant differences between strains. In the control 824(pSOS95del) strain, acetone and butanol are the primary solvents produced, 109 and 176 mM, respectively, while ethanol formation is relatively minor, at ca. 20 mM. The acetone production of 824(pCASAAD) is slightly higher than in 824(pAADB1), but 824(pSOS95del) produces twice the acetone of 824(pCASAAD). Butanol production was higher in 824(pCASAAD) (178 mM) and 824(pSOS95del) than in 824(pAADB1) (146 mM). Significantly, butanol was produced earlier and reached its final levels in half the time in 824(pCASAAD) (ca. 60 h) than in 824(pSOS95del) (ca. 120 h) (Fig. 2). Ethanol production was dramatically higher in 824(pCASAAD) and 824(pAADB1) than in 824(pSOS95del). 824(pCASAAD) produced 305 mM ethanol, 15 times higher than the control strain, while 824(pAADB1) produces 184 mM. This is the highest ethanol production reported by any solventogenic clostridium. These data show that butyryl-CoA and acetyl-CoA are important determinants of solvent yields and selectivities; this and the earlier butanol formation are better demonstrated by metabolic flux analysis as presented next.

Metabolic Flux Analysis of the Three Strains Supports the Limiting Role of Butyryl-CoA and Acetyl-CoA for Butanol Versus Ethanol Production, Respectively

Intracellular fluxes for 824(pAADB1) and 824(pCASAAD) were calculated and normalized both for differences in lag times of growth and cell density (Desai et al., 1999a). Butanol and ethanol fluxes show significantly higher values early in 824(pCASAAD) than in 824(pAADB1) or the plasmid control, 824(pSOS95del). This is consistent with the observation that the FDNH fluxes ($NADH_2$ production from reduced ferredoxin; Fig. 1) showed higher values earlier in the order (high to low) of 824(pCASAAD), 824(pAADB1) and 824(pSOSdel). In strain 824(pCASAAD), the butanol formation flux dropped to less than 25% its maximum at 21 h, while the ethanol formation flux was maintained at over 50% its maximal value for nearly 60 h. Although the peak formation values occur later in 824(pAADB1), the same trends in butanol and ethanol production were evident. In 824(pAADB1), the ethanol flux reached its maximum value after the butanol formation flux sharply decreased at 25 h. Butanol formation preceded ethanol formation in all strains, but ethanol formation was sustained for longer time periods than butanol formation, and especially so after 25 h when the flux (BYCA) to butyryl-CoA as well as the acetate and butyrate fluxes were largely reduced to zero, while the GLY 2 flux (Fig. 1) remained still at reasonable levels (ca. 1 mM A_{600}^{-1} h^{-1}; data not shown). This suggests that butyryl-CoA availability limits butanol formation, while the substantial flux to acetyl-CoA combined with high levels of AAD expression feeds and sustains the flux to ethanol at high levels thus leading to the very high ethanol titers. The nearly zero flux of acetate formation after 25 h and the sustained high ethanol fluxes late past 50–60 h suggest that the high AAD activity combined with the likely lower activities of the acetate formation enzymes (based on transcriptional information, data not shown) are responsible for channeling most of the carbon to ethanol by utilizing all the available reducing power, and thus the zero H_2 formation flux (rHYD) at that time period (data not shown).

Table II. Product formation in pH 5.0 fermentation experiments: effect of *aad* expression from the *ptb* promoter.

	Fermentation characteristics[a]							
Strains	Max A_{600}	Butanol	Ethanol	Acetone	$Acetate_{peak}$	$Acetate_{final}$	$Butyrate_{peak}$	$Butyrate_{final}$
824(pSOS95del)	5.79	176	19	109	80	77	73	37
824(pAADB1)	5.60	146	184	42	147	129	53	1
824(pCASAAD)	11.80	178	300	61	105	85	20	2

[a]All results shown are average mM concentration from duplicate experiments.

The butyrate formation flux is particularly low in 824(pCASAAD), thus demonstrating that the strategy for channeling butyryl-CoA from butyrate to butanol formation by the early and strong *aad* overexpression has worked as anticipated. Due to the low butyrate formation, butyrate uptake is much lower in 824(pCASAAD). Acetate formation is also sustained better and longer in 824(pAADB1) than in 824(pCASAAD) and the plasmid-control strain, and this is consistent with the deduced longer sustained acetyl-CoA pool. Comparing the acid uptake fluxes with the acetone formation flux, it is evident that acetone is produced almost solely from the uptake of acetate, as the acetate uptake flux is 10-fold higher than the butyrate uptake flux in both 824(pAADB1) and 824(pCASAAD). Acetone formation is also sustained longer in 824(pAADB1) than in 824(pCASAAD), but both strains show the anticipated lower acetone fluxes compared to 824(pSOS95del) as a result of the asRNA dowregulation of the acetone-formation enzyme CoAT.

Role of Thiolase Promoter and Thiolase Expression on the Acetyl-CoA to Butyryl-CoA Flux, and Its Impact on Product Formation

The data discussed above (Figs. 2 and 3) suggest that there exists a bottleneck for the formation of butyryl-CoA from acetyl-CoA. Four enzymes catalyze the conversion of butyryl-CoA from acetyl-CoA (Fig. 1). These are organized into two operons on the chromosome. The first enzyme in the pathway, thiolase (coded by the monocistronic *thl*), converts acetyl-CoA to acetoacetyl-CoA. The other three enzymes, β-hydroxybutyryl-coenzyme A dehydrogenase (BHBD), crotonase (CRO), and butyryl-CoA dehydrogenase (BCD), convert acetoacetyl-CoA to butyryl-CoA and are coded by genes which are co-transcribed on a single polycistronic transcript from a large operon (Boynton et al., 1996). *thl* is expressed at high levels and its constitutive-like expression (Tummala et al., 1999) makes it an ideal

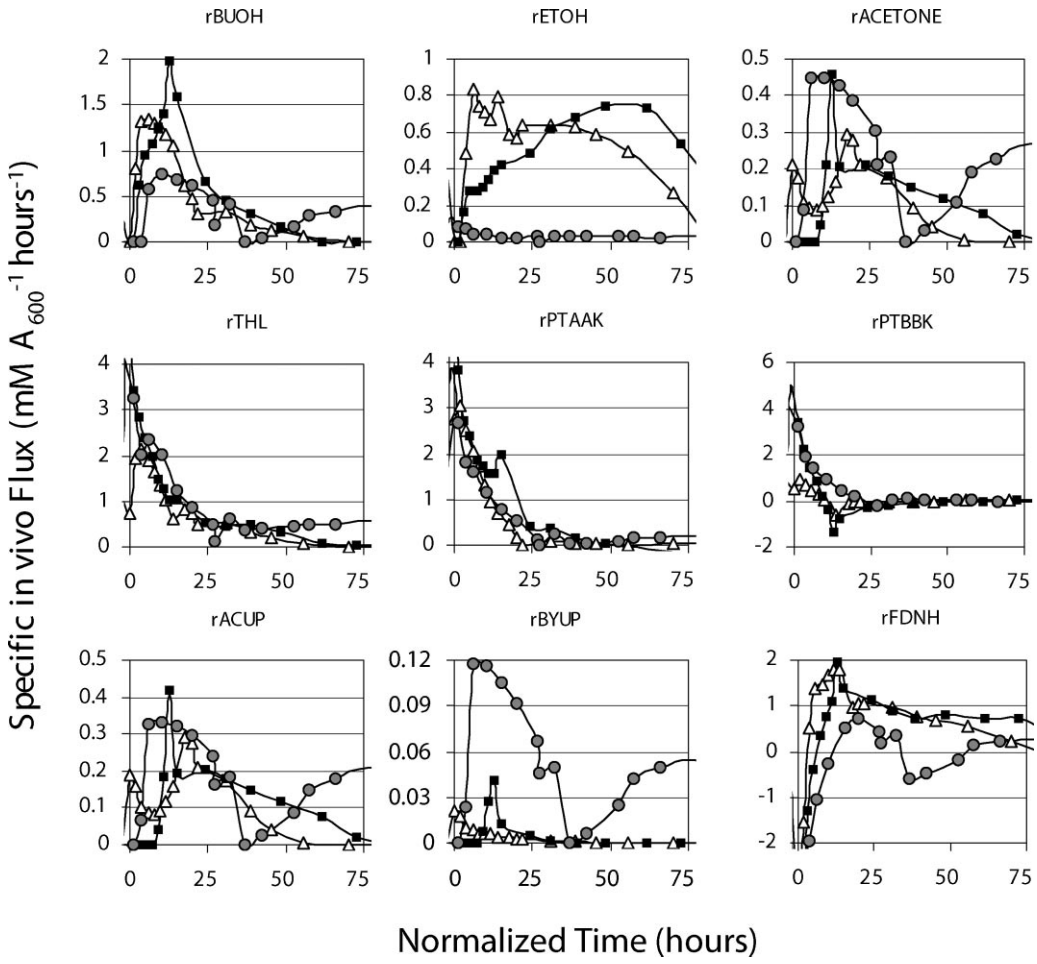

Figure 3. Metabolic flux analysis of 824(pCASAAD), 824(pAADB1), and 824(pSOS95del). 824(pCASAAD) results are shown as open triangles, 824(pAADB1) results are shown as closed squares, and 824(pSOS95del) results are shown as gray circles. Lag times were standardized between fermentations by normalizing an A_{600} of 1.0 at hour 10 of the fermentation.

promoter (p_{thl}) for high expression studies in clostridia, and was thus used to drive the expression of the *ctfB* asRNA in these studies. It is possible that the use of p_{thl} for the *ctfB* asRNA could have lowered the expression of the endogenous *thl* gene due to promoter titration effects, thereby lowering THL activity and creating the acetyl-CoA buildup. In order to test this hypothesis, the *ctfB* asRNA was expressed from another promoter, namely the promoter of the acetoacetate decarboxylase (Fig. 1) gene *adc* (p_{adc}), which is also highly expressed but later than *thl* (Tummala et al., 1999). Since p_{adc} is used in the formation of acetone, any promoter titration effects would not negatively impact butanol formation. A 100-basepair oligonucleotide was designed to include the integral portions of the *adc* promoter (Gerischer and Dürre, 1990). Following its ligation into the pIMP1 shuttle vector, another oligonucleotide was designed to include the Shine-Delgarno sequence of the *ctfB* gene and ca. 50 basepairs of the downstream coding sequence. Following the *ctfB* sequence was the *glnA* hairpin terminator (Desai and Papoutsakis, 1999). This new *ctfB* asRNA was ligated downstream of p_{adc} to create plasmid pCAS (Table I), which was transformed into the WT strain to confirm the functionality of the new *ctfB* asRNA. Strain 824(pCAS) was characterized in static fermentations and compared to the original *ctfB* asRNA. Acetone formation was much lower in 824(pCAS) than in the 824(pSOS95del) control strain (Table III). 824(pCAS) fermentations also displayed low overall solvent formation and higher acid formation with limited acid reassimilation compared to 824(pSOS95del). These results are consistent with the previous *ctfB* asRNA strain (Tummala et al., 2003a,b).

To determine if low THL levels were limiting the conversion of acetyl-CoA to butyryl-CoA in the WT strain without *aad* overexpression, the *thl* gene including its endogenous promoter was amplified from genomic DNA and ligated into the pIMP1 shuttle vector to create plasmid pTHL. Following the transformation of this plasmid into the WT strain, pH-controlled bioreactor experiments were used to characterize the strain. The metabolism of the 824(pTHL) is characterized by initial levels of high acid production, typical in clostridial fermentations, but there is only very limited acid reassimilation (Table III). Along with the elevated levels of acid production, there is a dramatic decrease in the levels of solvents produced. Additionally, there is a sharp decrease in the cell density of the culture and a plateau of the glucose uptake just a few hours following the peak butyrate production. This may indicate that the cells cannot reassimilate butyrate promptly and the solvent genes cannot be induced to respond to the butyrate production, which leads to growth inhibition. We hypothesized that *aad* overexpression using p_{ptb} would promote early butanol production and a means for preventing the accumulation of inhibitory butyrate concentrations.

Overexpression of *aad* using p_{ptb} was analyzed with (strain 824(pTHLAAD)) and without (strain 824(pPTBAAD)) *thl* overexpression, and the fermentation data are summarized in Table III. As a result of *aad* overexpression, ethanol levels in 824(pPTBAAD) increased to 76 mM, more than three times the WT production. Additionally butyrate was nearly completely re-assimilated by this strain, while the final butanol titer was 160 mM. Acetate production in 824(pPTBAAD) was also very high reaching final levels of 124 mM. With the addition of *thl* overexpression, 824(pTHLAAD) shows a significant shift in product formation compared to 824(pPTBAAD). Ethanol production is reduced from 76 mM in 824(pPTBAAD) to 28 mM in 824(pTHLAAD). Acetate formation in 824(pTHLAAD) is also reduced to nearly half the level of 824(pPTBAAD). Butanol is produced at similar levels in both strains while *thl* overexpression causes a small increase in butyrate formation. Acetone levels were ca. 40% higher in 824(pTHLAAD) compared to 824(pPTBAAD).

Comparing the profiles of the different fluxes (Fig. 4) provides additional insight into the role of *thl* overexpression. Consistent with the *thl* overexpression, there is an increase in the thiolase flux in 824(pTHLAAD) from about 5 to 30 h (notice that the time scale in the flux analysis is in normalized hours) compared to 824(pPTBAAD). The higher butanol and BYCA fluxes early (in normalized hours) in the fermentation show that butanol is produced earlier in 824(pTHLAAD) than in 824(pPTBAAD) apparently because *thl* overexpression can enhance the butyryl-CoA rate of formation. The ethanol formation flux is similar between the two strains until about 25 h into the fermentation when the flux is sharply reduced to zero at 40 h in 824(pTHLAAD), while the ethanol formation flux is

Table III. Product formation in pH 5.0 fermentation experiments: effect of thiolase expression.

	Fermentation characteristics[a]							
Strains	Max A_{600}	Butanol	Ethanol	Acetone	$Acetate_{peak}$	$Acetate_{final}$	$Butyrate_{peak}$	$Butyrate_{final}$
824(pTHL)	10.67	54	6	34	68	68	76	71
824(pTHLAAD)	9.75	153	28	98	68	67	39	17
824(pPTBAAD)	11.90	160	76	59	124	124	62	2
824(pCAS)[b]	3.59	53	11	29	38	38	45	34
824(pSOS95del)[b]	4.35	152	21	91	22	12	33	22

[a]All results shown are average mM concentration from duplicate experiments.
[b]Results are from static flask experiments without pH control.

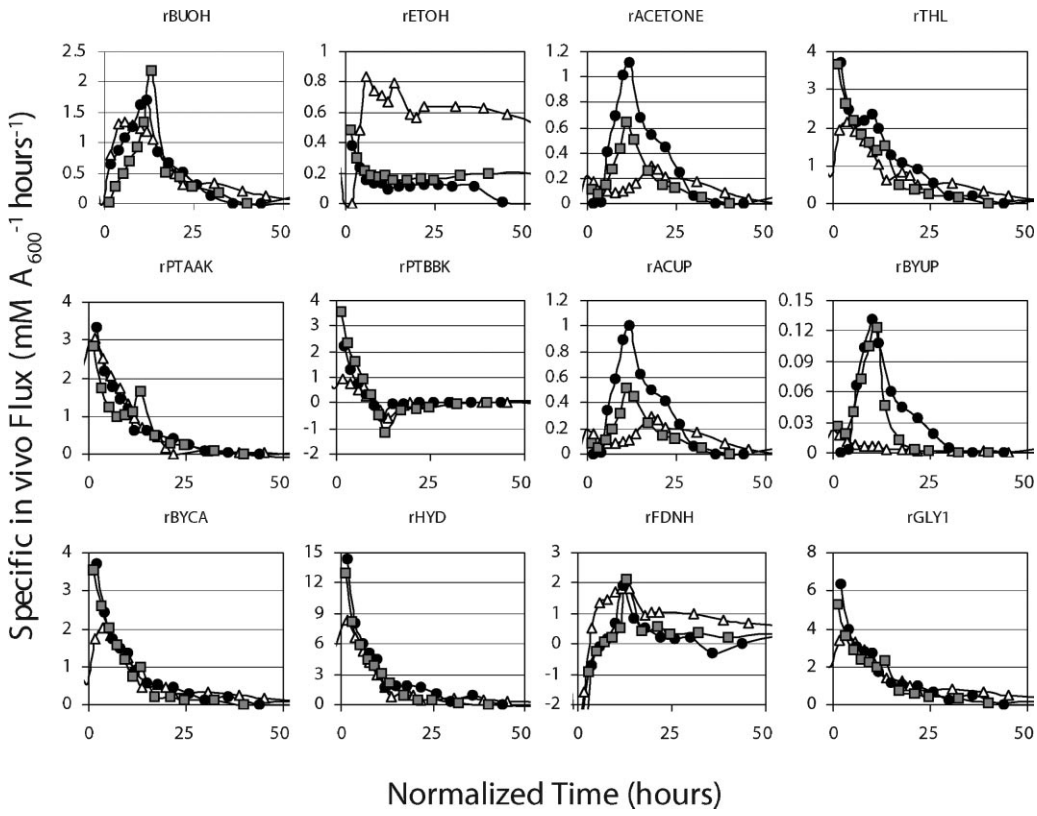

Figure 4. Metabolic flux analysis of 824(pTHLAAD), 824(pPTBAAD), and 824(pCASAAD). 824(pTHLAAD) results are shown as closed circles, 824(pPTBAAD) results are shown as grey squares, and 824(pCASAAD) results are shown as open triangles. Lag times were standardized between fermentations by normalizing an A_{600} of 1.0 at hour 10 of the fermentation.

sustained at a high level in 824(pPTBAAD) after 50 h. The HYD and FDNH fluxes are not affected by *thl* overexpression. Comparing the acid formation fluxes there appears to be little difference, but the acid uptake fluxes are significantly increased in 824(pTHLAAD) compared with 824(pPTBAAD): the acetate uptake flux is nearly twice as high in 824(pTHLAAD) and is sustained longer than in 824(pPTBAAD), while the butyrate uptake flux has a similar magnitude, but is sustained longer in 824(pTHLAAD). The acetone formation flux follows a similar pattern as the acetate uptake flux showing that acetone formation is mostly due to acetate uptake. Significantly, except for the first few hours, the BYCA flux is identical between the two strains. These flux analysis data then show that *thl* overexpression enhances acetoacetyl-CoA formation, which enhances acetone formation and acetate uptake. Except for very early in the fermentation (in normalized hours), the lack of a major impact on the BYCA flux suggests that that flux is limited by one of the BHBD, CRO or BCD enzymes (Fig. 1).

Thus, *thl* overexpression achieved in principle the goal of reducing the acetyl-CoA pool and thus reduce the formation of ethanol and acetate. Indeed, in 824(pPTBAAD) the ratio of the concentrations of the four carbon products (butanol and butyrate) to the two carbon products (ethanol and acetate) was 0.81. When *thl* was overexpressed with *aad* in 824(pTHLAAD), this ratio more than doubled to 1.79.

A comparison of the fermentation data from strains 824(pPTBAAD) and 824(pCASAAD) (Tables II and III) illuminates the impact of the asRNA CoAT downregulation. This is analyzed in detail below.

The Combined Effect of *thl* and *aad* Overexpression With CoAT Downregulation

Plasmid pSS2 (Table I) was constructed to combine *thl*, *aad* (from the p_{ptb}) overexpression, and CoAT downregulation by asRNA, but for the latter using the p_{adc} instead of the p_{thl} used in the pCASAAD and pAADB1 plasmids. pH controlled bioreactor experiments of strain 824(pSS2) were once again used to characterize the strain in order to compare to the 824(pCASAAD) and 824(pTHLAAD) strains (Fig. 5). Strain 824(pSS2) grew more slowly than either 824(pCASAAD) or 824(pTHLAAD) and product formation was delayed even when normalized for differences in lag times; this is probably due to a general metabolic burden by the larger plasmid. Peak acetate production in 824(pSS2) was similar to 824(pCASAAD), but final acetate

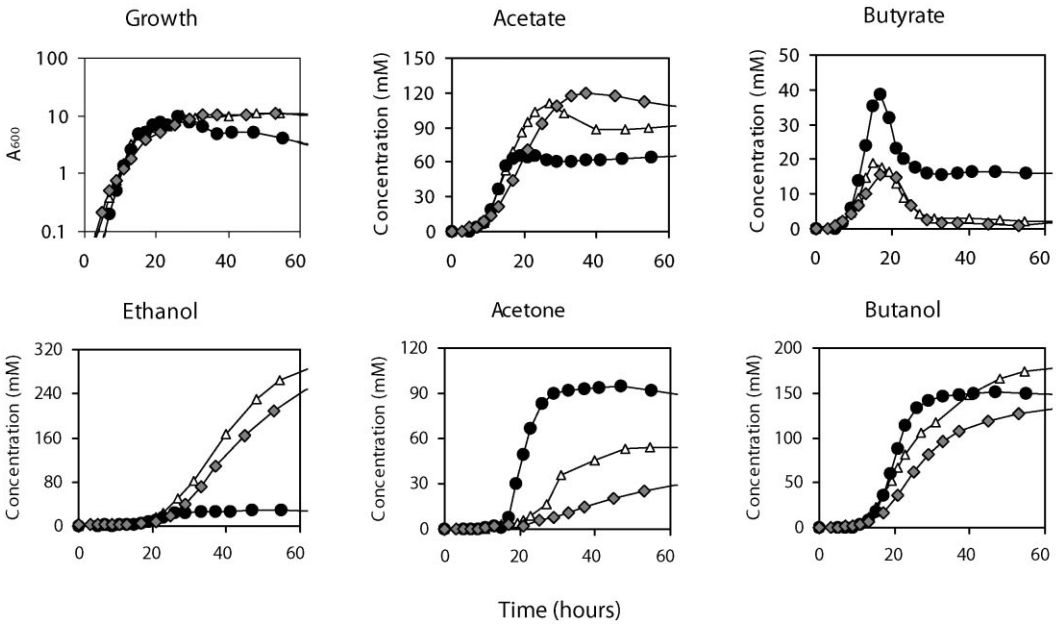

Figure 5. Growth and product concentrations of 824(pCASAAD), 824(pTHLAAD), and 824(pSS2) pH 5.0 fermentations. Fermentations were performed in duplicate, while results are shown from one fermentation. Differences in product formation between duplicate fermentations are less than 5%. Lag times were standardized between fermentations by normalizing an A_{600} of 1.0 at hour 10 of the fermentation. 824(pCASAAD) results are shown as open triangles, 824(pTHLAAD) results are shown as closed circles, and 824(pSS2) results are shown as gray diamonds.

concentrations were higher. Butyrate formation in 824(pSS2) was similar to that in 824(pCASAAD), which has lower peak and final butyrate levels than 824(pTHLAAD). Ethanol formation at 288 mM was very high in 824(pSS2), nearly as high as in 824(pCASAAD), which is much greater than ethanol production in 824(pTHLAAD). Acetone levels are much lower in the two strains harboring the *ctfB* asRNA, while butanol levels were fairly similar across all strains with the lowest levels achieved in 824(pSS2).

824(pSS2) shows a more similar profile to 824(pCASAAD), which does not overexpress *thl* (but produces somewhat higher butanol and acetone levels) than 824(pTHLAAD), which does overexpress *thl*. These results indicate that *ctfB* asRNA combined with *aad* overexpression provide the dominant phenotype (high butanol and ethanol formation with suppressed acetone formation), which additional *thl* expression is unable to modulate in terms of enhancing butanol formation. It can be also argued that p_{adc} driven asRNA CoAT downregulation has the desirable outcome, namely in producing a large suppression of acetone formation (which is fractionally larger than the suppression of either butanol or ethanol formation; compare the profiles of strain 824(pSS2) and 824(pCASAAD) in Fig. 5).

If one compares strains 824(pSS2) and 824(pTHLAAD), the impact of CoAT downregulation in the former is expected in that it reduces acetone formation, but unexpected in that it dramatically enhances ethanol and acetate formation apparently due to an increased acetyl-CoA pool. The same conclusion is drawn when one compares strains 824(pPTBAAD) and 824(pCASAAD) (Tables II and III): CoAT downregulation enhances dramatically ethanol formation but is accompanied by a lower final acetate production. An explanation of these phenotypic difference is a bit more complex thus necessitating a comparison of the fluxes between these two strains is shown in Figure 4 pCASAAD has much higher ethanol and butanol formation fluxes, lower rTHL fluxes, dramatically lower acetate (rACUP) and butyrate (rBYUP) uptake fluxes, altered rFDNH, and altered acetate formation fluxes (higher early, lower later), all of which point to altered regulation around the acetyl-CoA node.

Discussion

We altered the pattern of *aad* expression by replacing the endogenous promoter with that of *ptb*, which is responsible for butyrate formation. This caused both earlier and higher expression of *aad* and had dramatic effects on the fermentation products (Fig. 2). All the solvents (acetone, butanol, and ethanol) were produced at higher levels in 824(pCASAAD) with p_{ptb} driven *aad* expression than in 824(pAADB1), which uses the native *aad* promoter. *ctfB* asRNA kept acetone concentrations low, while ethanol concentrations reached the highest levels observed with this organism. The total amount of solvents produced by 824(pCASAAD) was over 30 g/L with 13–14 g/L each of butanol and ethanol. WT fermentations produce only about

20 g/L solvents, but acetone and butanol are the primary products. Additionally, butyrate is not totally reassimilated by the WT strain as it is in 824(pCASAAD). Final acid levels can be 15–25% of the total products in WT *C. acetobutylicum* fermentations, but in 824(pCASAAD) fermentations acids are only 5–10% of the total products. Other high solvent producing clostridia strains have been engineered that produced between 25 and 29 g/L total solvents in batch cultures, but again, the primary products are butanol and acetone (Harris et al., 2000; Qureshi and Blaschek, 2001; Tomas et al., 2003c). With the emergence of biofuels, strains producing ethanol may be preferred over those producing acetone as other significant products.

Metabolic flux analysis showed that the earlier expression of *aad* resulted in earlier formation of both butanol and ethanol. It also appears that butyryl-CoA depletion may lead to the high ethanol yields. Ethanol production only becomes significant as butanol production decreases due to reduced availability of butyryl-CoA. As the same enzyme (AAD; Fig. 1) catalyzes butanol and ethanol formation, genomic manipulations to directly decrease ethanol formation cannot be achieved by a simple metabolic engineering strategy. To further increase the butanol titers one must divert more of the acetyl-CoA (the precursor of ethanol) to butyryl-CoA. Thiolase (THL) is the first enzyme in the conversion of acetyl-CoA to butyryl-CoA and its role in solvent production was investigated. *thl* overexpression combined with *aad* overexpression lowered production of acetate and ethanol, while increasing acetone and butyrate levels. The *ctfB* asRNA used in the earlier studies was also redesigned to eliminate the use of the *thl* promoter to alleviate concerns of transcription factor titration effects. Although the combined *thl* and *aad* overexpression does produce a substantial shift in the fermentation products, the combination of *thl* and *aad* overexpression with CoAT asRNA downregulation did not significantly alter product formation compared to the strain without *thl* overexpression. This indicates that with fewer genetic manipulations, *thl* gene dosage may be an important contributor to the final end products, but the combination of *ctfB* asRNA and *aad* overexpression may result in internal metabolite concentrations too constrained for *thl* overexpression to impart any benefit. In particular, the BYCA flux appears resistant to change by *thl* overexpression (Fig. 5; compare strain 824(pSS2) to strain 824(pCASAAD); flux data are not shown), thus possibly necessitating the overexpression of one of the BHBD, CRO or BCD enzymes (Fig. 1). This is a rather complex undertaking for two reasons: first, the size of the plasmid required for overexpressing some or all of these genes together and the genes or asRNAs already on plasmids pSS2 or pCASAAD will be very large and will impose a large metabolic burden on the cells. Second, it is not clear which of the three genes of the BYCA linear pathway is rate limiting and especially because additional electron transport proteins may be necessary (Boynton et al., 1996). Nevertheless, this is a problem we plan to pursue in our lab in the quest for better strains to produce butanol. At the same time, a fresh approach is necessary in order to be able to exercise control over the ratio of butanol to ethanol produced.

This work is supported by a National Science Foundation grant (BES-0418157). We thank Abbott Laboratories for the donation of clarithromycin. We also thank Dr. Ryan Senger for the development of the software used during the metabolic flux analysis.

References

Alsaker KV, Papoutsakis ET. 2005. Transcriptional program of early sporulation and stationary-phase events in *Clostridium acetobutylicum*. J Bacteriol 187(20):7103–7118.

Alsaker KV, Spitzer TR, Papoutsakis ET. 2004. Transcriptional analysis of spo0A overexpression in *Clostridium acetobutylicum* and its effect on the cell's response to butanol stress. J Bacteriol 186(7):1959–1971.

Alsaker K, Paredes CJ, Papoutsakis ET. 2005. Design, optimization, and validation of genomic DNA microarrays for examining the *Clostridium acetobutylicum* transcriptome. Biotechnol Bioprocess Eng 10(5):432–443.

Boynton ZL, Bennett GN, Rudolph FB. 1996. Cloning, sequencing, and expression of clustered genes encoding β-hydroxybutyryl-coenzyme A (CoA) dehydrogenase, crotonase, and butyryl-CoA dehydrogenase from *Clostridium acetobutylicum* ATCC 824. J Bacteriol 178(11): 3015–3024.

Clark SW, Bennett GN, Rudolph FB. 1989. Isolation and characterization of mutants of *Clostridium acetobutylicum* ATCC 824 deficient in acetoacetyl-coenzyme A:acetate/butyrate:coenzyme A-transferase (EC 2.8.3.9) and in other solvent pathway enzymes. Appl Environ Microbiol 55(4):970–976.

Cornillot E, Nair RV, Papoutsakis ET, Soucaille P. 1997. The genes for butanol and acetone formation in *Clostridium acetobutylicum* ATCC 824 reside on a large plasmid whose loss leads to degeneration of the strain. J Bacteriol 179(17):5442–5447.

Desai RP, Papoutsakis ET. 1999. Antisense RNA strategies for metabolic engineering of *Clostridium acetobutylicum*. Appl Environ Microbiol 65(3):936–945.

Desai RP, Harris LM, Welker NE, Papoutsakis ET. 1999a. Metabolic flux analysis elucidates the importance of the acid-formation pathways in regulating solvent production by *Clostridium acetobutylicum*. Metab Eng 1(3):206–213.

Desai RP, Nielsen LN, Papoutsakis ET. 1999b. Metabolic flux analysis of *C. acetobutylicum* fermentations using nonlinear constraints. J Biotechnol 71:191–205.

Gerischer U, Dürre P. 1990. Cloning, sequencing, and molecular analysis of the acetoacetate decarboxylase gene region from *Clostridium acetobutylicum*. J Bacteriol 172(12):6907–6918.

Harris LM, Desai RP, Welker NE, Papoutsakis ET. 2000. Characterization of recombinant strains of the *Clostridium acetobutylicum* butyrate kinase inactivation mutant: Need for new phenomenological models for solventogenesis and butanol inhibition? Biotechnol Bioeng 67(1): 1–11.

Harris LM, Welker NE, Papoutsakis ET. 2002. Northern, morphological, and fermentation analysis of *spo0A* inactivation and overexpression in *Clostridium acetobutylicum* ATCC 824. J Bacteriol 184(13):3586–3597.

Heap JT, Pennington OJ, Cartman ST, Carter GP, Minton NP. 2007. The ClosTron: A universal gene knock-out system for the genus Clostridium. J Microbiol Methods 70(3):452–464.

Husemann MHW, Papoutsakis ET. 1988. Solventogenesis in Clostridium-Acetobutylicum fermentations related to carboxylic-acid and proton concentrations. Biotechnol Bioeng 32(7):843–852.

Mermelstein LD, Papoutsakis ET. 1993. In vivo methylation in *Escherichia coli* by the *Bacillus subtilis* phage phi 3T I methyltransferase to protect plasmids from restriction upon transformation of *Clostridium acetobutylicum* ATCC 824. Appl Environ Microbiol 59(4):107710–107781.

Mermelstein LD, Welker NE, Bennett GN, Papoutsakis ET. 1992. Expression of cloned homologous fermentative genes in *Clostridium acetobutylicum* ATCC 824. Biotechnology (NY) 10(2):190–195.

Nair RV, Bennett GN, Papoutsakis ET. 1994. Molecular characterization of an aldehyde/alcohol dehydrogenase gene from Clostridium-Acetobutylicum Atcc-824. J Bacteriol 176(3):871–885.

Nölling J, Breton G, Omelchenko MV, Makarova KS, Zeng Q, Gibson R, Lee HM, Dubois J, Qiu D, Hitti J, Wolf YI, Tatusov RL, Sabathe F, Doucette-Stamm L, Soucaille P, Daly MJ, Bennett GN, Koonin EV, Smith DR. 2001. Genome sequence and comparative analysis of the solvent-producing bacterium *Clostridium acetobutylicum*. J Bacteriol 183(6):4823–4838.

Qureshi N, Blaschek HP. 2001. Recent advances in ABE fermentation: Hyper-butanol producing Clostridium beijerinckii BA101. J Ind Microbiol Biotechnol 27(5):287–291.

Shao L, Hu S, Yang Y, Gu Y, Chen J, Yang Y, Jiang W, Yang S. 2007. Targeted gene disruption by use of a group II intron (targetron) vector in *Clostridium acetobutylicum*. Cell Res 17(11):963–965.

Tomas CA, Alsaker KV, Bonarius HPJ, Hendriksen WT, Yang H, Beamish JA, Parades CJ, Papoutsakis ET. 2003a. DNA-array based transcriptional analysis of asporogenous, non-solventogenic *Clostridium acetobutylicum* strains SKO1 and M5. J Bacteriol 185(15):4539–4547.

Tomas CA, Beamish JA, Papoutsakis ET. 2003b. Transcriptional analysis of butanol stress and tolerance in *Clostridium acetobutylicum*. J Bacteriol 186(7):2006–2018.

Tomas CA, Welker NE, Papoutsakis ET. 2003c. Overexpression of *groESL* in *Clostridium acetobutylicum* results in increased solvent production and tolerance, prolonged metabolism, and large changes in the cell's transcriptional program. Appl Environ Microbiol 69(8):4951–4965.

Tummala SB, Welker NE, Papoutsakis ET. 1999. Development and characterization of a gene expression reporter system for *Clostridium acetobutylicum* ATCC 824. Appl Environ Microbiol 65(9):3793–3799.

Tummala SB, Junne SG, Papoutsakis ET. 2003a. Antisense RNA downregulation of coenzyme A transferase combined with alcohol-aldehyde dehydrogenase overexpression leads to predominantly alcohologenic *Clostridium acetobutylicum* fermentations. J Bacteriol 185(12):3644–3653.

Tummala SB, Welker NE, Papoutsakis ET. 2003b. Design of antisense RNA constructs for downregulation of the acetone formation pathway of *Clostridium acetobutylicum*. J Bacteriol 185(6):1923–1934.

Zhao YS, Tomas CA, Rudolph FB, Papoutsakis ET, Bennett GN. 2005. Intracellular butyryl phosphate and acetyl phosphate concentrations in *Clostridium acetobutylicum* and their implications for solvent formation. Appl Environ Microbiol 71(1):530–537.